ELECTROSTATIC HINDRANCE TO DIFFUSION IN FLEXIBLE CROSSLINKED GELS: A COARSE-GRAINED SIMULATION STUDY

Luis Pérez-Mas[1], María del Mar Ramos-Tejada[1], Alberto Martín-Molina[2,3*], José-Alberto Maroto-Centeno[1] and Manuel Quesada-Pérez[1]

[1]Departamento de Física, Escuela Politécnica Superior de Linares, Universidad de Jaén, 23700, Linares, Jaén, Spain.

Emails: lpmas@ujaen.es , mmramos@ujaen.es, jamaroto@ujaen.es, mquesada@ujaen.es,

[2]Departamento de Física Aplicada, Universidad de Granada, Campus de Fuentenueva s/n, 18071 Granada, Spain.

Email: almartin@ugr.es

[3]Instituto Carlos I de Física Teórica y Computacional, Universidad de Granada, Campus de Fuentenueva s/n, 18071 Granada, Spain

(*) Corresponding author

ABSTRACT

In this work, we study how electrostatic forces slow down the diffusion of solute in flexible gels through coarse-grained simulations. The model used explicitly considers the movement of solute particles and polyelectrolyte chains. These movements are performed by following a Brownian Dynamics algorithm. The effect of three electrostatic parameters characterizing the system (solute charge, polyelectrolyte chain charge and ionic strength) is analyzed. Our results show that the behavior of both the diffusion coefficient and the anomalous diffusion exponent changes upon reversal of the electric charge of one of the species. In addition, the diffusion coefficient in flexible gels differs significantly from that in rigid gels if the ionic strength is low enough. However, the effect of chain flexibility on the exponent of anomalous diffusion is significant even at high ionic strength (100 mM). Our simulations also prove that varying the polyelectrolyte chain charge does not have exactly the same effect as varying the solute particle charge.

INTRODUCTION

Diffusion through polymer gels plays a key role in many technological processes, such as water purification,[1] drug delivery[2,3] or tissue engineering.[3] In many of these applications, both the polymer network and the particles that diffuse through it (drugs, nutrients, proteins, etc.) have electrical charge, and it is well known that electrostatic interactions can modulate the diffusivity and permeability of these gels. We can find a good example of this in mucus, a polymer-based hydrogel covering the inner linings of the body that constitutes a protective barrier against viruses, bacteria, and toxic agents. Recent research on mucus has proven that electrostatic interactions between traversing particles and this hydrogel govern to a great extent its filtering capacity.[4] Strongly interacting particles are retained by the hydrogel, whereas weakly interacting particles manage to pass through the mucus. Therefore, it is interesting to achieve a better understanding of how electrostatic forces regulate the diffusivity and permeability of biological and technological charged hydrogels.

The first researchers who tried to shed light on this matter at the early nineties with the help of a coarse-grained model were Johansson and Löfroth. [5] They considered point-like monovalent ions diffusing through ordered and disordered rigid charged networks. The ordered networks were modelled as parallel straight chains whereas randomly oriented worm-like chains were employed for the disorder ones. In both cases, polyelectrolyte chains consisted of charged spherical beads. The electrostatic forces between monovalent ions and these beads were included in the model through the screened Debye-Hückel interaction potential.

Some years later, Miyata et al. simulated the diffusion of a moderately charged nanoparticle (instead of monovalent ions) in oppositely charged network made of static beads arranged along the sides of a cubic lattice.[6,7] The attractive electrostatic interaction

between the nanoparticle and the beads forming the network was considered through the expression derived by Wiese and Healy, which is also a screened interaction potential. One of the most outstanding results of these coarse-grained simulations was the immobilization of the nanoparticle if the electrostatic attractive forces are intense enough. Stylianopoulos et al. simulated the diffusive movement of a particle through an array of rigid parallel fibers with charge of the same sign.[8] Steric, electrostatic and hydrodynamics interactions were considered. These researchers concluded that repulsive electrostatic interactions slow down solute diffusion if the fiber size is of the same order as the Debye screening length.

More recently, Hansing et al. have simulated solute diffusion in charged gels.[9,10] They modelled the polymer network as infinite rigid rods in the three directions of space (forming a cubic lattice). Their systematic study is advisable and includes both attractive and repulsive electrostatic forces. They concluded that electrostatic forces always slow down the diffusive motion of the solute. In other words, these forces always represent an additional obstruction to diffusion. However, such electrostatic obstruction is charge asymmetric. This means that diffusion is slowed down much more by electrostatic attraction than by repulsion. In later works, Hasing et al. considered certain disorder in the polymer network and hydrodynamic interactions in their model.[11,12]

In summary, previous coarse-grained simulations confirm that electrostatic interactions greatly influence solute diffusion in charged gels. It should be pointed out, however, that such simulations only considered static (and therefore rigid) polymer networks. Thus, the main goal of this work is to find out to what extent diffusive properties of flexible charged gels differs from those of the rigid charged ones. Our model also considers polymeric chains composed of spherical beads, as Johansson and Miyata did.[5–7] In addition, we also employ a screened electrostatic potential. However, unlike much of the previous work,

polymer chains can change their shape because their monomeric units can move under some restrictions. In other words, the flexibility of polymer chains is taken into account. Coarse-grained models are an idealization of reality. Nevertheless, their simplicity is also their biggest advantage. Since the constituents of these models and the interactions between them are perfectly known, it is possible to assess their effects without the interference of unknown aspects. In fact, the effect of flexibility on diffusion through ideal uncharged polymer networks has already assessed with the help of coarse-grained simulations.[13,14] Other issues on diffusion within flexible polymer networks have also been addressed through this kind of simulations in recent years. For instance, some researchers have simulated the movement of solute particles through polymer networks when the particle size is comparable to the mesh size or larger.[15–18] Others have considered different polymer-solute interactions or polydispersity in polymer gels.[19–22] Finally, other applications of coarse-grained models include the use of polyelectrolyte gels as a tool for specific viral detection[23] or the adsorption of polyelectrolyte chains onto Janus nanoparticles.[24]

Accordingly, the aim of this work is to investigate the role of electrostatic interactions in solute diffusion through charged flexible gels. To this end, coarse-grained simulations are performed to calculate diffusion coefficients. The charge of the solute particle and the chains that form the network as well as the ionic strength are varied. Structural properties of the systems are also analyzed in order to shed light on the underlying physical mechanisms. Lastly, the effect of the polymer stiffness and interaction forces on the anomalous diffusion regime is examined. The rest of the paper is organized as follows. First, the model used and the simulations carried out are described in some detail. Then, results are presented. Finally, some conclusions are highlighted.

MODEL AND SIMULATIONS

In the coarse-grained model employed here, each monomeric unit of the polymer chain is simulated by a sphere (or bead). All chains have the same number of monomeric units and their ends are chemically bonded by crosslinking molecules, which are also modelled as spherical beads. Many crosslinkers used in the synthesis of polymer and polyelectrolyte gels are tetrafunctional (e.g., *N*,*N*'-methylenebisacrylamide), which means that they are linked to four chains. Solute particles are also modelled as spheres. Both solute particles and monomeric units can have electric charge. Neither solvent molecules (water in this case) nor small ions are explicitly considered in this model.

Excluded-volume (steric) interactions between any pair of beads are modelled though hard sphere potentials. The forces between chemically bonded beads (monomeric units and crosslinking molecules), which provide structural stability to the network, are assumed to obey Hooke's law. Therefore, the potential energy of interaction (U_{bond}) is given by:

$$U_{bond}(r_{ij}) = \frac{1}{2} k_{bond}(r_{ij} - r_0)^2 \qquad (1)$$

Here r_{ij} is the center-to-center distance between interacting beads i and j, k_{bond} is the elastic constant and r_0 is the equilibrium length of this harmonic potential.

In addition, the electrostatic interaction between charged beads are included in the model through the screened Debye-Hückel interaction potential:

$$U_{elec}(r_{ij}) = \lambda_B k_B T Z_i Z_j \frac{\exp(\kappa R_i)}{1+\kappa R_i} \frac{\exp(\kappa R_j)}{1+\kappa R_j} \frac{\exp(-\kappa r_{ij})}{r_{ij}} \qquad (2)$$

In this expression, λ_B denotes the so-called Bjerrum length, k_B is Boltzmann's constant, T is the absolute temperature, Z_i and R_i are the number of elementary charges (which we will also refer to as charge number) and the radius, respectively, of bead i, and κ is the Debye screening parameter, which can be computed as $\kappa = \sqrt{8\pi\lambda_B N_A I}$, where I is the

ionic strength (in mM) within the gel and N_A is Avogadro's number. The interaction potential given by Equation 2 is similar to that employed by Johansson and Löfroth.[5] One of the limitations of this potential is that it was derived from linear approximations in the Poisson-Boltzmann theory. This means that Equation 2 is strictly valid for very small electrostatic potentials (less than 25 mV in absolute value), which in turn implies very low charges. However, it is well known that Equation 2 can be used beyond this limit if ions are monovalent and the charges appearing in it are replaced by renormalized charges.[25] Therefore, hereafter we will assume that the charges used in this work are renormalized rather than the actual ones. In relation to Equation 2, it should also be mentioned that it does not consider the effect of image charges. Cherstvy and Winkler studied the effect of image charges on the polyelectrolyte adsorption onto oppositely charged interfaces.[26] If the tracer particle has a low electric permittivity (such as mica or polymeric particles), an electrostatic repulsion from image charges of the same sign created beneath the interface should be taken into account in addition to the direct polyelectrolyte-surface electrostatic attraction.

The following are the values of the model parameters used here. The diameter of monomeric units and crosslinkers is 0.60 nm. The size of many real monomers is of this order.[27] Each polyelectrolyte chain is formed by 10 monomeric units, which corresponds to a moderately crosslinked network. The diameter of the beads representing solute particles is 1.00 nm. Many drug molecules have mean diameters in this range (e.g., doxorubicin[28]). The polymer volume fraction is 0.01 in all cases. In this way, steric obstruction is almost negligible and the effect of flexibility on electrostatic obstruction can be easily identified. Regarding the elastic interaction between bonded beads, $k_{bond} =$ 0.4 N/m and $r_0 = 0.6$ nm. These values guarantee the structural stability of the network and the proximity between neighboring monomeric units. $Z_i = -1,0,+1$ for monomeric

units and varies from −6 to +6 for solute particles. Crosslinkers are not charged. Simulations have been performed at 293 K ($\lambda_B = 0.71$ nm in water at this temperature) and two ionic strengths: 10 and 100 mM. These two I-values are sufficient to observe under which electrolytic conditions the effect of flexibility on electrostatic obstruction is important.

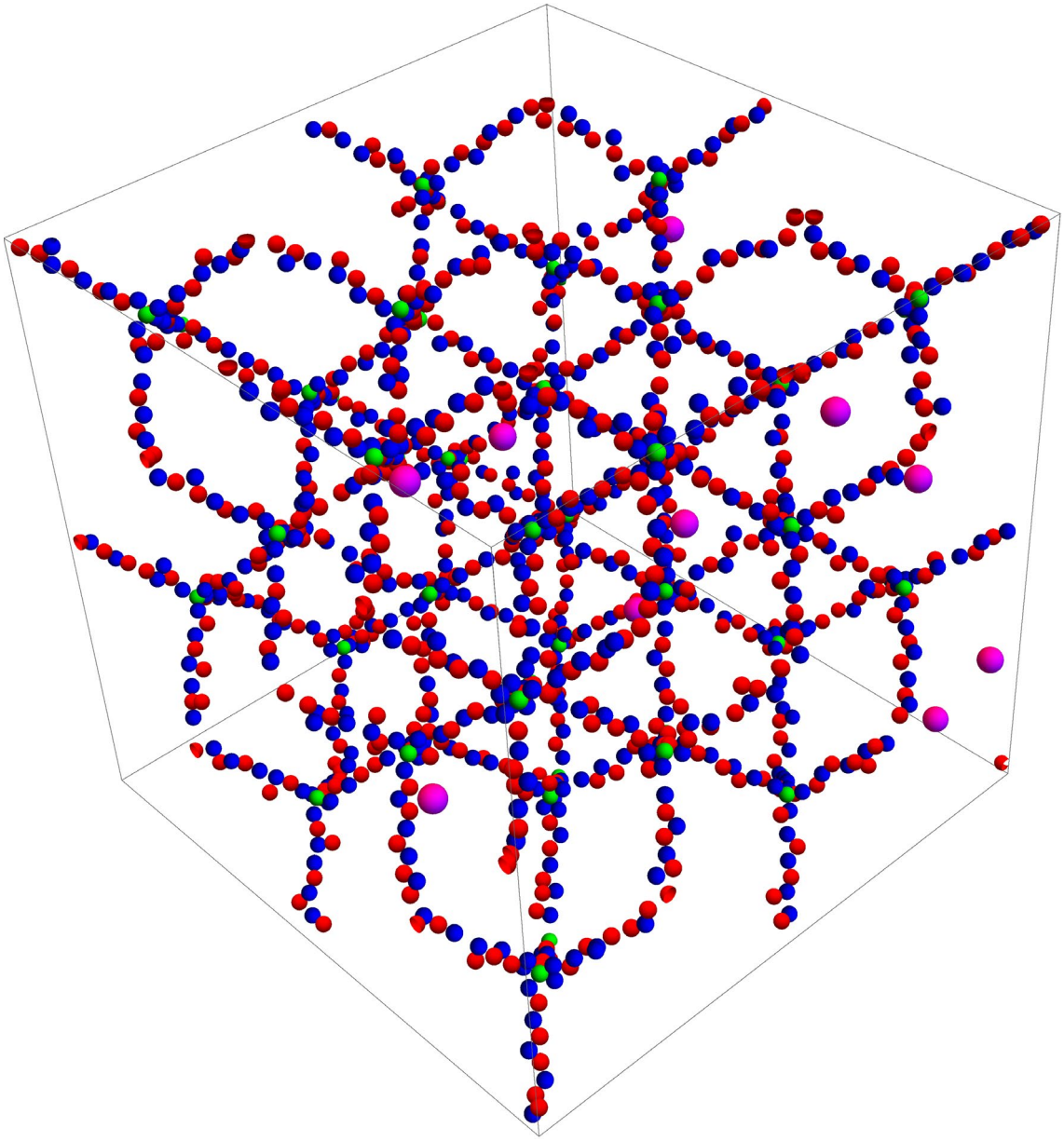

Figure 1. Snapshot of the simulation box used for gels at 10 mM just after thermalization. Green, blue, red and magenta beads represent crosslinking molecules, neutral monomeric units, charged monomeric units and solute particles, respectively. The mean distance between nearest crosslinking molecules is about 5.5 nm.

The simulation box is a cube of side L replicated in the three spatial directions through periodic boundary conditions. The dimensions of this cube and the number of beads that it contains depends on the ionic strength so that the effect of electrostatic forces of the replicated cells (beyond the minimum image convention) is negligible. In fact, according to the criterion adopted here, $L/2$ must be at least four times larger than the Debye length ($L/2 > 4\kappa^{-1}$). In addition, L must be adjusted to reproduce the desired polymer volume fraction. For 100 mM, the simulation box contains 8 crosslinkers, 160 monomeric units (16 polymer chains) and one solute particle. Its length is 12.4 nm. For 10 mM, L is double and the volume is eight times greater. Therefore, the numbers of crosslinkers and monomeric units must also be multiplied by eight so that the polymer volume fraction remains constant. The number of solute particles is not subject to such a severe restriction. However, it seems reasonable to multiply by a similar factor. Figure 1 displays the simulation box for 10 mM.

Initially, the crosslinkers are placed forming a diamond-like lattice and the monomeric units are arranged along the straight lines that join them. Before simulating solute diffusion, the polymer network must evolve from its initial configuration to a state representative of equilibrium. This thermalization process is carried out by means of Monte Carlo (MC) simulation (5000 MC steps per bead were performed). The diffusive motion of solute begins after reaching an equilibrium configuration. In the case of rigid gels, this configuration of the polymer network remains fixed and only the drug molecules move. In contrast, in the case of flexible gels, the monomeric units and crosslinkers that make up the network also move. In either of these two cases, these movements are executed following a Brownian dynamics algorithm (adapted to hard spheres).

In the absence of hydrodynamic interactions, the Cartesian components of the displacement vector of particle i during a time step Δt are given by:[29]

$$\Delta r_{mi} = \sqrt{2D_{0i}\Delta t}N(0,1) + D_{0i}F_{mi}\Delta t/k_BT \quad (3)$$

In this expression, m denotes the spatial directions (x, y or z), D_{0i} is the free diffusion coefficient of particle i in the solvent (which can be estimated from the Einstein-Stokes relationship), $N(0,1)$ is a random number generated according to a Gaussian distribution of zero mean and unit standard deviation, and F_{mi} is the Cartesian m-component of the net force exerted on particle i. Elastic and electrostatic forces are calculated as the negative of the gradient of Equations (1) and (2). However, the hard sphere potential is not differentiable. Consequently, excluded-volume interactions has been included in the algorithm following the strategy used by Cichocki and Hinsen:[30] the displacement vector given by Equation 3 is provisional and will be rejected if it leads to the overlapping of beads. The time step employed in these simulations was 3.0 ps. This value was chosen after certain preliminary tests taking into account that: i) the results could depend on this parameter if it is not small enough; ii) very short time steps yield extremely time-consuming simulations.

RESULTS

1. Diffusion coefficients.

As mentioned previously, our study is focused on electrostatic obstruction to diffusion. If the ionic force remains constant, electrostatic forces can be modified by varying the charge of the particle or the charge of the chains that form the network. Both possibilities are explored in our simulations. Table 1 shows the solute charge number (Z_S) and the chain charge number (Z_C) of the two types of series performed here: variable solute charge (VSC) series and variable chain charge (VCC) series. Z_C is varied by modifying the number of charged beads per chain. Figure 2 shows where the charged monomeric

units are located for different Z_C-values. It should be noted that charge distributions are discrete and non-uniform in these cases.

Table 1. Parameters of the series simulated here.

Type of series	Solute charge number (Z_S)	Chain charge number (Z_C)	Ionic strength (mM)	Type of gel
Variable solute charge (VSC)	–6, –5, –4, –3, –1, 0, +1, +3. +4, +5, +6	+10	100, 10	Rigid and flexible gels
Variable chain charge (VCC)	–6	+9. +8, +5, +2, +1, 0, –1, –2. –5, –8, –9	100, 10	Rigid and flexible gels

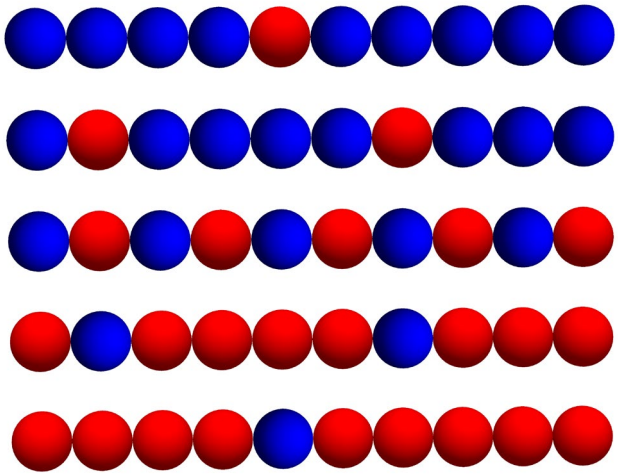

Figure 2. Relative positions of the charged monomeric units in the polyelectrolyte chains for chain charge numbers (Z_C) ±1, ±2, ±5, ±8, ±9 (from top to bottom).

The main output of our simulations is the mean square displacement (MSD) of solute particles, $\langle \Delta r^2 \rangle$, which was computed averaging on 300 independent solute particle trajectories. Figure 3 displays the MSD as a function of time corresponding to the series VSC, 10 mM, flexible gels (just as an example). This figure also includes the line corresponding to free diffusion for comparison. As can be seen, all the curves deviate downwards with respect to the line of free diffusion. Such deviations are small for $Z_S = \pm 1$ but significant for the rest of solute charges. In any case, this means that the motion of the solute particle is slower in the presence of electrostatic interactions. Nevertheless,

it is worth comparing MSDs corresponding to charges of the same magnitude but opposite sign. As can be concluded, the deviations from the free diffusion line are larger when solute and chains are oppositely charged, which confirms that the electrostatic obstruction is charge asymmetric. This log-log plot also shows that, if time (t) is long enough, the MSD curves are parallel to the free diffusion line. In other words: at long times, the MSD ends up reaching a diffusive regime. In fact, the proportionality constant between the MSD and time provides us the diffusion coefficient of the solute within the gel (D): $D = \langle \Delta r^2 \rangle / 6t$ (evaluated at the end of the simulation after averaging). However, before reaching this diffusive regime, the MSD exhibits a transient regime where this function is proportional to t^n (with $n < 1$), which is known as subdiffusive regime or anomalous diffusion.[31–33]

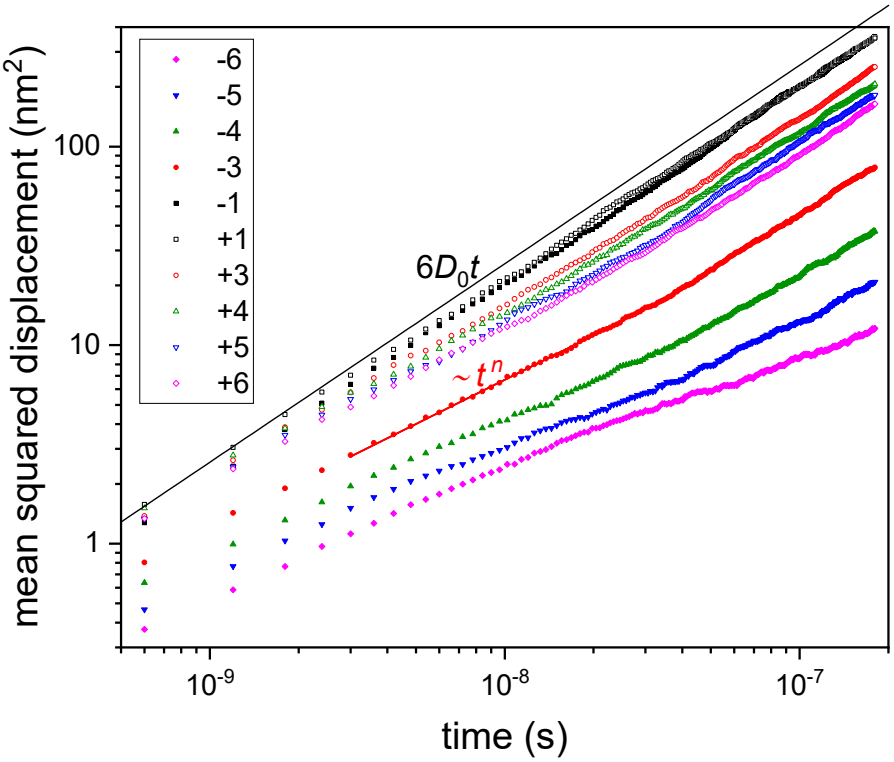

Figure 3. Mean squared displacement as a function of time for different solute charge numbers. The gel is flexible, its polymer volume fraction is 0.01 and the charge number of its chains is +10. The ionic strength is 10 mM. The line corresponding to free diffusion is also plotted for comparison (black line). The red line represents the regime in which the MSD is proportional to t^n for a solute charge number of −3.

At this point, let us focus on the diffusive regime at long times. Figure 4 displays the relative diffusivity (D/D_0, where D_0 stands for the free diffusion coefficient of the solute) at 100 mM for VSC and VCC series as well as for flexible and rigid gels in both series. Each simulation was repeated three times to obtain the mean value and the standard deviation of the diffusion coefficient. The resulting data are plotted as a function of the product of charges, $Z_S Z_C$. In this way, VSC and VCC series can be represented in the same graph. Hansing et al. plotted their results as a function of the product of the charge of the solute, the linear charge density of the rods of their model, and a sphere-cylinder geometrical factor that characterizes the interaction between the solute and the rods.[10] In our case, polyelectrolyte chains are not modelled as straight rods and no analytical

expression provides such a geometrical factor. For that reason, this factor is not included in our electrostatic parameter.

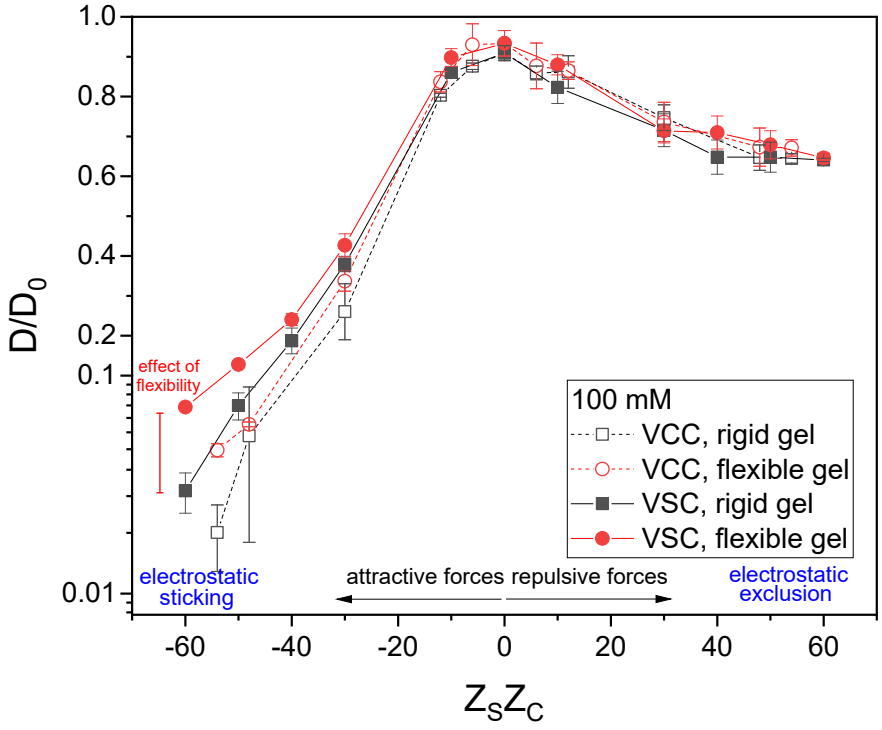

Figure 4. Relative diffusivity at 100 mM as a function of the product of charge numbers, $Z_S Z_C$. The graph includes series corresponding to variable chain charge (VCC) and variable solute charge (VSC) in flexible and rigid gels. It should be noted that the *y*-axis is logarithmic below 0.1.

As can be seen in Figure 4, the relative diffusivity is less than unity for both positive and negative values of the product $Z_S Z_C$. This confirms again that electrostatic interactions imply an obstruction to diffusion for both repulsive and attractive forces. However, this obstruction is more intense if the gel and the solute are oppositely charged. Hansing *et al.* reached this conclusion for a rigid cubic lattice.[9,10] Our data confirm it for flexible networks, more disordered and of different topology. It is easy to understand why the attractive forces between the solute and the polymer network reduce the diffusion coefficient. Such forces cause sticking, i.e. the solute particle tends to remain near the polymer chains,[10] which considerably hinder their movement. In contrast, repulsive

forces keep solute particles away from polymer chains. Why then do they also reduce the diffusion coefficient? Electrostatic repulsive forces prevent solute particles from approaching the polymer chains. This implies a reduction in their accessible volume, whose effects are expected to be similar to an increase in the volume fraction.

In any case, the model used here allows us to reach conclusions that go beyond the mere confirmation or extension of previous results. For instance, the comparison between flexible and rigid gels reveals that chain flexibility is not important at 100 mM (except for $Z_S Z_C = -60$) since no significant differences are observed in the series corresponding to flexible and static networks. However, some differences are found between the VSC and VCC curves for negative values of the product of charges. In this region, the VCC curves fall below the VSC curves. Remember that in the VCC case, the charge is not evenly distributed along the chain. This suggests that non-uniform charge distributions hinder solute diffusion more efficiently. Why does this only happen for attractive electrostatic forces? As mentioned before, electrostatic repulsive forces keep solute particles away from the polyelectrolyte chains and the effects of charge heterogeneities are much smaller (and even negligible) at long distances.

As previously mentioned, Figure 4 suggests that gels with non-uniform charge distributions slow down solute diffusion more efficiently. In the case of chains with only one or two charged monomeric units, the question arises as to whether the relative position of the charged monomers affects diffusion. In order to answer this question, let us consider chains with $Z_C = +1$ at 100 mM. We have assumed that the charge is located in the fifth monomeric unit, right in the middle of the chain (see Figure 2). Figure 5 shows what happens if the charged monomer is placed in other relative positions on the chain. As can be seen, the relative diffusion is significantly reduced when the charged monomer moves away from the center of the chain. This decrease in relative diffusion is similar for

flexible and rigid gels. If the electric charge is at one end of the chain, the relative diffusion drops to 0.6. This noticeable reduction in the relative diffusion can be attributed to the accumulation of charged monomers around some crosslinkers, which considerably increases the probability of sticking.

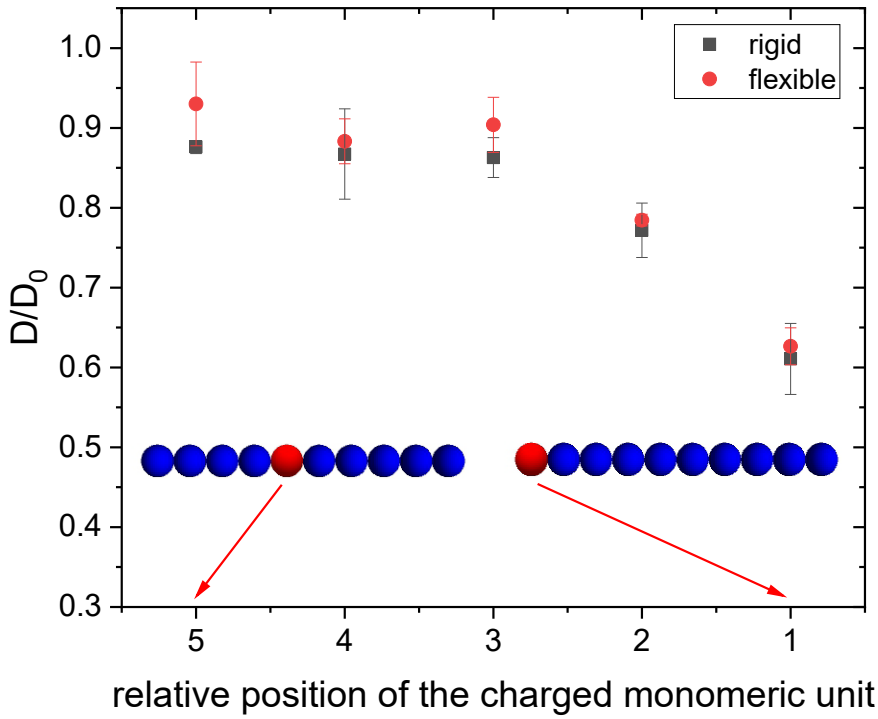

Figure 5. Relative diffusivity in rigid and flexible gels with $Z_C = +1$ at 100 mM as a function of the relative position of the charged monomeric unit.

Figure 6 displays the VSC and VCC series (for flexible and rigid gels) at 10 mM. In general, an intensification of electrostatic obstruction is observed in both sides of the graph (positive and negative $Z_S Z_C$-values). The sticking produced by attractive forces is now much stronger. In fact, the extremely low values of relative diffusivity suggest that solute particles are almost immobilized in some cases. On the other hand, the exclusion due to repulsive forces is also more intense, which enhances the electrostatic obstruction

for $Z_S Z_C > 0$, although to a lesser extent. Consequently, diffusion continue being charge asymmetric.

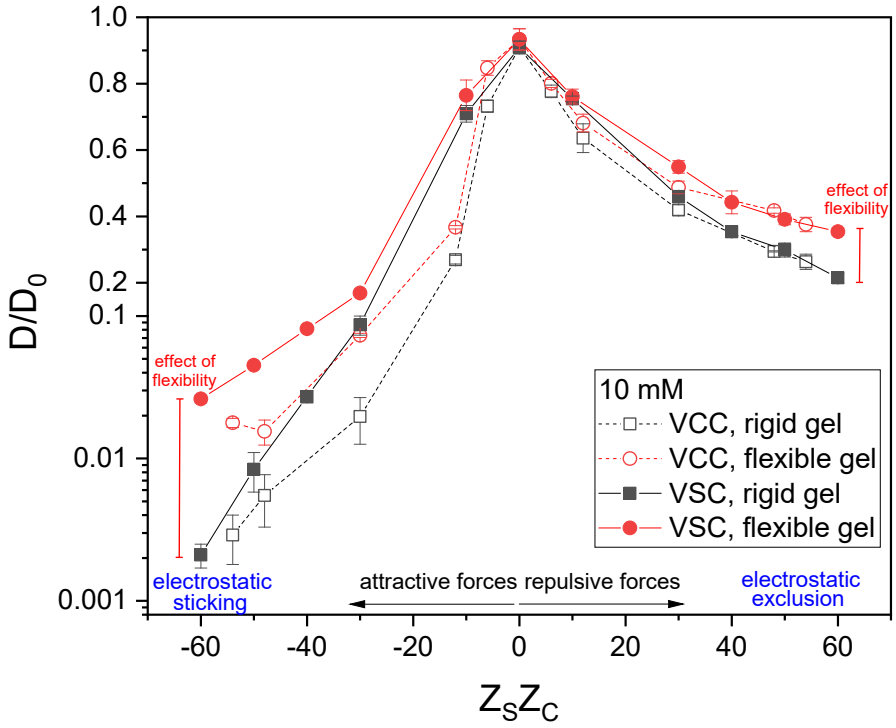

Figure 6. Relative diffusivity at 10 mM as a function of the product of charge numbers, $Z_S Z_C$. The graph includes series corresponding to variable chain charge (VCC) and variable solute charge (VSC) in flexible and rigid gels. It should be noted that the *y*-axis is logarithmic below 0.1.

Apart from that, the comparison between data corresponding to flexible and rigid gels reveals that the flexibility of the polyelectrolyte chains now has significant effects. Flexibility facilitates solute diffusion in the presence of both repulsive and attractive forces. At the far right of the graph ($Z_S Z_C = +60$), the relative diffusivity in flexible gels is 60% greater than in the rigid ones. On the far left ($Z_S Z_C = -60$), the diffusion coefficient increases by one order of magnitude.

It is also interesting to compare VSC and VCC series. In the region of repulsive forces, the differences between them are negligible again. In the case of attractive forces, the electrostatic obstruction is greater for VCC series, whose charge distributions are not

uniform. This behavior, which is similar to that reported for 100 mM, confirms that the product $Z_S Z_C$ is not sufficient to fully and unambiguously characterize the electrostatic obstruction to diffusion in flexible gels. Regarding the left half of Figure 6, it should also be noted that, for small negative $Z_S Z_C$-values, the relative diffusivity decreases more rapidly in the VCC series. In fact, this parameter drops below 0.4 for $Z_C = +2$. This sharp decrease can be attributed to the charge accumulation around crosslinkers, as discussed in Figure 5.

It should also be mentioned that the VCC series for flexible gels includes a dot on its left end that might draw the attention of some readers. As can be seen, the relative diffusivity of $Z_S Z_C = -54$ is slightly larger than that of $Z_S Z_C = -48$. This breaks the general trend that electrostatic obstruction increases with charge. Given the error bars of the dot with $Z_S Z_C = -48$, it could be a mere statistical deviation.

The asymmetry in charge reported from simulations has been observed in experiments with Alexa488 (a negatively charged fluorescent molecule) diffusing through positively and negatively charged dextran hydrogels.[34] Since the experimental conditions of this work and our simulation parameters do not match, a precise quantitative comparison between simulation and experiment is not possible. However, some rough similarities can be found. For example, the relative diffusivity in positively charged gels increases from approximately 0.1 to 0.8 when the ionic strength changes from 20 to 100 mM. An increase of the same order of magnitude is observed in Figures 4 and 6 for $Z_S Z_C \approx -15$ in the VCC series of rigid gels when the ionic strength varies from 10 to 100 mM. In the case of negatively charged hydrogels, the relative diffusivity remains almost constant as the ionic strength is varied, with values close to 0.8. This is also observed in our data for $Z_S Z_C \approx +7$ (again in the VCC series of rigid gels), suggesting that positive dextran

hydrogels are more highly charged than negative dextran hydrogels. Hansing *et al*. came to the same conclusion. [10]

2. Radial distribution functions and Gaussian behavior.

As mentioned above, the comparison of Figure 4 and Figure 6 reveals that the effects of flexibility on electrostatic hindrance are greater at 10 mM. This seems logical, since the forces on charged deformable polymer chains are stronger at low ionic strengths. To further investigate the effects of flexibility under such conditions and the underlying mechanisms, additional information will be analyzed in four representative cases at 10 mM: $Z_S Z_C = +60$ in flexible gel; $Z_S Z_C = +60$ in rigid gel; $Z_S Z_C = -60$ in flexible gel; and $Z_S Z_C = -60$ in rigid gel. For short, we will refer to these cases as +60F, +60R, –60F and –60R, respectively. In some cases, however, results corresponding to 100 mM will also be plotted for comparison. Let us start with the spatial distribution of solute particles. Figure 7 displays the solute-charged-monomer and solute-crosslinker radial distribution functions ($g_{SM}(r)$ and $g_{SC}(r)$, respectively) corresponding to the four cases at 10 mM. For +60F and +60R (repulsive electrostatic forces between solute particles and polyelectrolyte chains), the radial distribution functions (rdfs) are null below certain r-values (1.7 nm in $g_{SM}(r)$ and 2.5 nm in $g_{SC}(r)$) and exhibit a pronounced peak at $r \approx 5$ nm. This confirms that solute particles are excluded from a certain region around charged monomers and crosslinkers and, in general, remain far away from them. A closer inspection of these functions also reveals that the height of the main peak and the amplitude of the subsequent oscillations are slightly larger for rigid gels. Consequently, the aforementioned exclusion is more intense in this case. This could explain why the stiffness of polymer chains contributes to electrostatic obstruction.

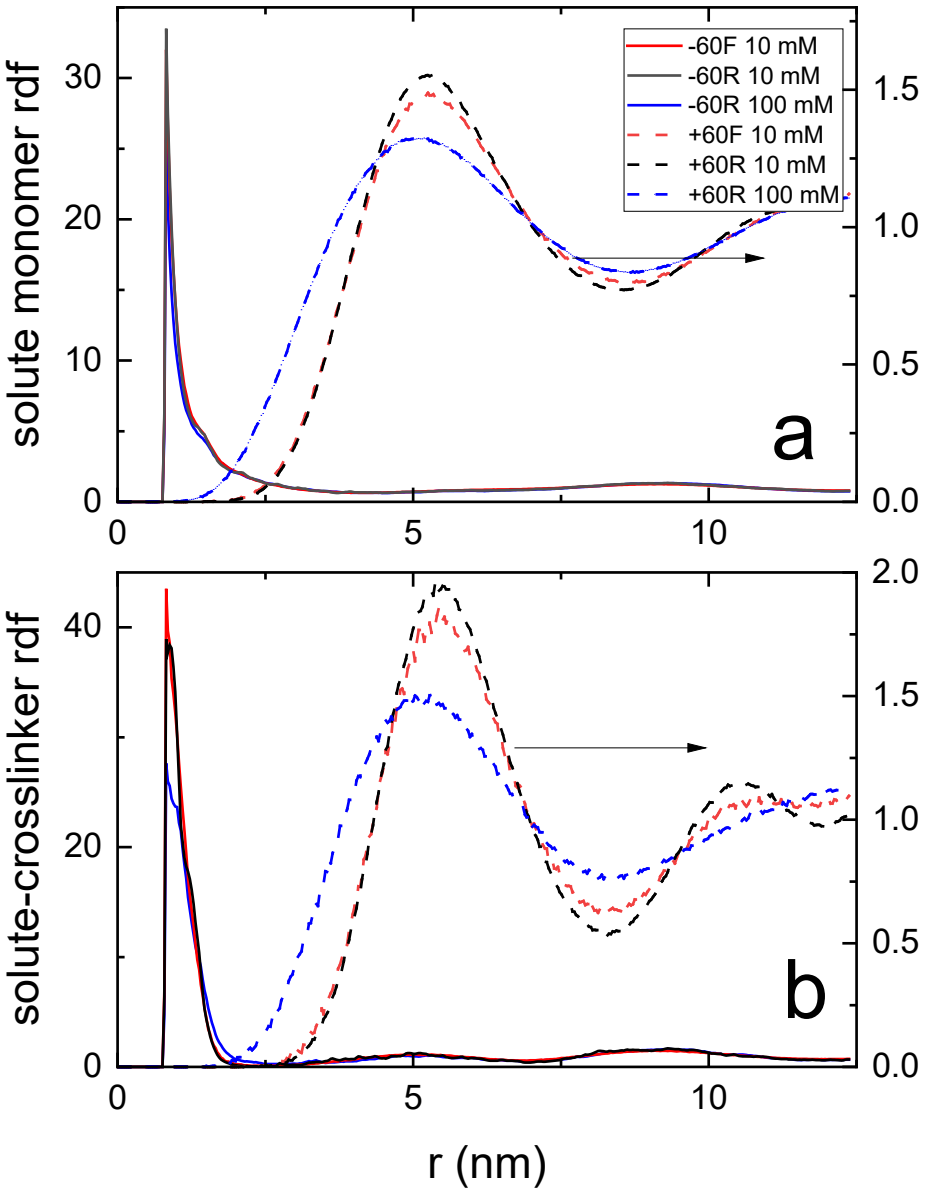

Figure 7. Charged-monomer-solute and crosslinker-solute radial distribution functions (plots a and b, respectively) as a function of the center-to-center distance between particles for cases +60F, +60R, –60F and –60R at 10 mM (dashed red line, dashed black line, solid red line and solid black line, respectively) and +60R and –60R at 100 mM (blue solid line and blue dashed line, respectively). Data corresponding to +60F and +60R are read on the right *y*-axis.

In the case of attractive forces (cases –60F and –60R), the solute-charged-monomer rdfs exhibit sharp peaks just at the contact distance between these two species (see Figure 7a),

which proves the existence of sticking between them. The height of the two main peaks of $g_{SM}(r)$ is almost identical. This suggests that the degree of sticking between charged monomeric units and solute particles is essentially the same for rigid and flexible networks.

A sharp peak is also observed in the solute-crosslinker rdf of flexible gels (Figure 7b). However, the peak corresponding to rigid networks is slightly lower. Probably the fixed monomers around crosslinkers prevent solute particles from approaching as closely as in the case of flexible gels. It should be kept in mind that the crosslinkers considered here do not carry electrical charge. Therefore, the presence of solute particles in close proximity to them should be attributed to the concentration of charged monomeric units in that region.

Figure 7 also includes rdfs for –60R and +60R at 100 mM for comparison. These simulations were exceptionally carried out in the 24.8 nm cell to cover larger distances. As can be seen, the peaks of the rdfs are lower at 100 mM than at 10 mM. This means electrostatic sticking and exclusion are weaker at 100 mM because the forces causing them are less intense. Figure 7 also shows that the peaks of +60R are shifted towards smaller r-values at 100 mM and the regions of total electrostatic exclusion ($g_{SM}(r) = 0$ and $g_{SC}(r) = 0$) are narrower.

At this point, we will focus our attention on the self-part of the Van Hove function ($P(\Delta x; t)$), which gives us the probability density that a particle moves Δx (in the x-direction) in a time t. This probability density has been computed for the four cases at 10 mM previously analyzed and is plotted as a function of Δx for three times (1200, 3000 and 30000 ps) in Figure 8. On a graph with linear axes, these functions resemble Gaussian distributions of different height and width. But, here, the y-axis is logarithmic to better appreciate their tails. In three of the four cases at 10 mM studied here (+60F, +60R and

–60F), it can be easily observed that the Van Hove functions lose height but gain width. This means that the solute particles wander in increasingly larger regions.

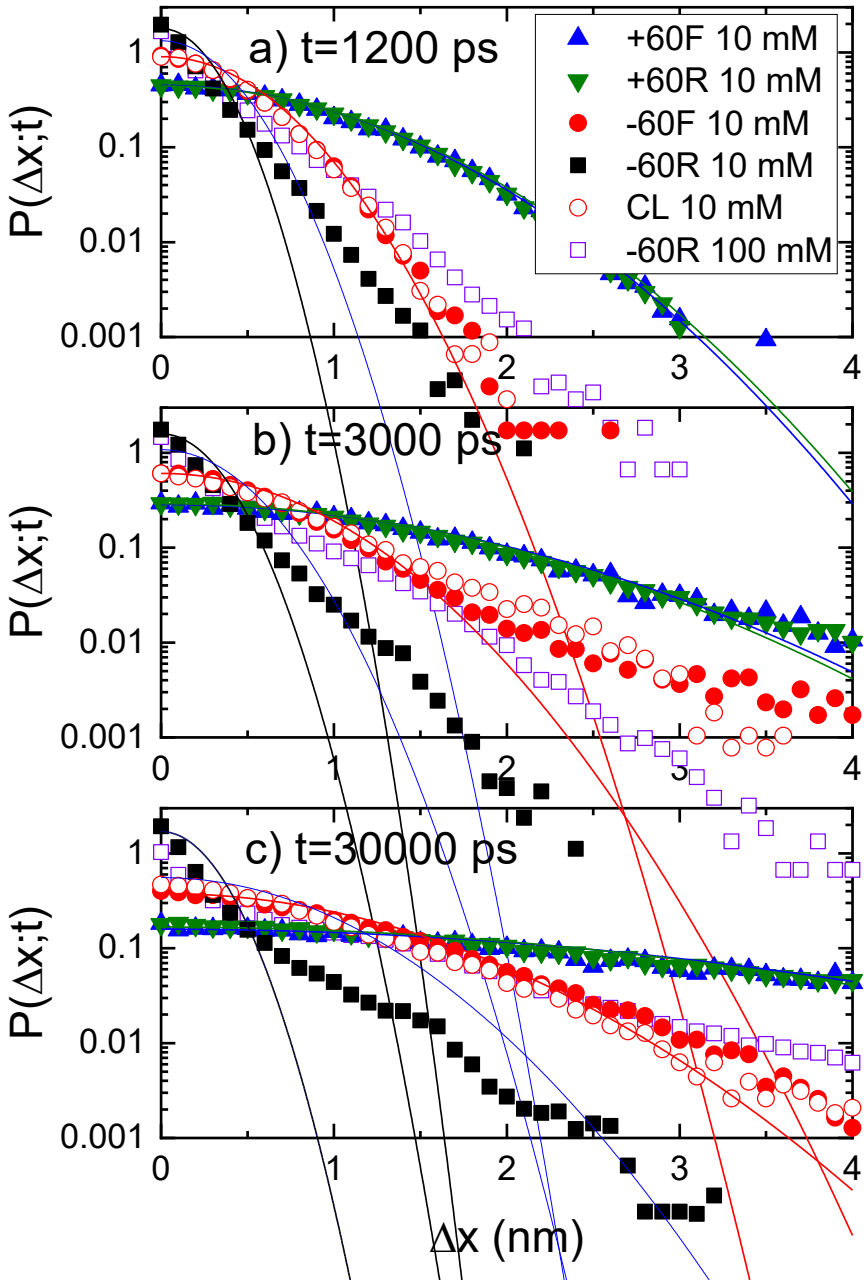

Figure 8. Self-part of the Van Hove function $P(\Delta x; t)$ of cases +60F, +60R, –60F and –60R at 10 mM (up triangles, down triangles, solid circles and squares, respectively) as a function of the x-component of displacement vector (Δx) at 1200, 3000 and 30000 ps (plots a, b and c, respectively). The functions corresponding to crosslinkers (CL) in –60F at 10 mM and –60R at 100 mM are also plotted for comparison (open red circles and open blue squares, respectively). Lines represent the best fits to a Gaussian distribution (Equation 4).

In the case of attractive electrostatic forces, the broadening of the Van Hove function is much slower, especially in the –60R case. This is not surprising because, according to its rdf, solute particles stick electrostatically to fixed crosslinkers. In flexible gels (–60F), they diffuse faster because they are bound to movable monomers and crosslinkers. The self-part of the Van Hove function corresponding to crosslinkers of –60F are also plotted in Figure 8 for comparison. As can be seen, this function is very similar to that of the solute (almost identical at 1200 ps). This means that, in this case, solute particles and the crosslinkers to which they stick move together much of the time.

Figure 8 also includes the Van Hove function of the –60R case at 100 mM. As can be seen, simulated distributions are wider at 100 mM than at 10 mM. In fact, the probability density of –60R at 100 mM is quite close to that of –60F at 10 mM. This means that multiplying the ionic strength by a factor of ten produces an effect of the same order of magnitude as giving flexibility to the network.

The self-part of the Van Hove function of a diffusive motion is a Gaussian distribution whose variance is proportional to time. To find out if the Van Hove functions represented in Figure 8 are Gaussian, they were fitted to the following normal distribution:

$$P(\Delta x; t) = \frac{1}{\sqrt{2\pi\langle \Delta x^2 \rangle}} \exp\left(\frac{-\Delta x^2}{2\langle \Delta x^2 \rangle}\right) \quad (4)$$

Here the brackets denote the ensemble average and $\langle \Delta x^2 \rangle$ is the only fitting parameter. As can be seen, the behavior of $P(\Delta x; t)$ is Gaussian if solute particles and polyelectrolyte chains have charges of the same sign (+60F and +60R). The behavior of –60F is also Gaussian to a large extent. It should be stressed, however, that deviations in the tail of the function are observed for long times and Δx greater to 2 nm. Since the solute particles are most likely bound to the crosslinkers, such large displacements would cause considerable

deformations in the polymer network. In fact, Kumar *et al*. attribute the deviations of $P(\Delta x; t)$ to stretching in the network.[35] It should also be mentioned that some of these large displacements can be of the order of the mean distance between crosslinkers (about 5 nm). Therefore, the solute might occasionally approach other crosslinkers and even jump to them. In that case, the solute could diffuse through the gel by hopping from crosslinker to crosslinker. One of these jumps is illustrated in Figure 9, which shows the trajectory of a solute particle (recorded every 600 ps). However, given the low probability of these jumps, diffusion would be very slow.

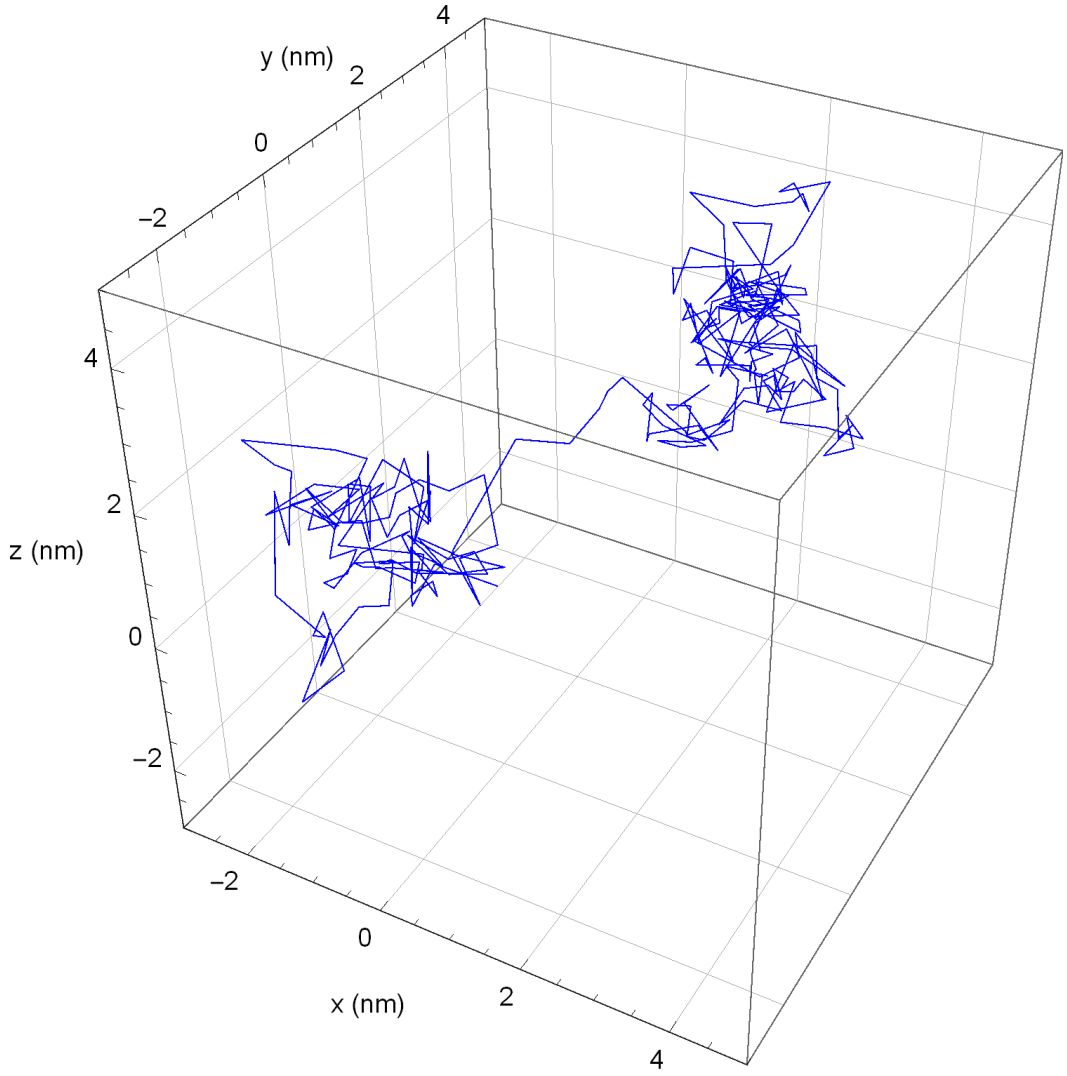

Figure 9. Trajectory of a solute particle (for case −60F at 10 mM) during a given iteration. Displacements were recorded every 600 ps. As can be seen, the solute particle spends most of its time in relatively small regions, but it occasionally changes places jumping from one crosslinker to another.

Let us return to the remaining cases of Figure 8 (–60R at 10 and 100 mM). The discrepancies between simulation data and the fits are so large for –60R that we must conclude that their displacements are not Gaussian and the solute motion is not purely diffusive. In addition, their extremely low diffusion coefficients must be carefully interpreted: solute particles remain trapped near crosslinkers.

The Gaussian character of the solute displacements can be corroborated with the help of the so-called non-Gaussian parameter (α_2), which is defined as:

$$\alpha_2 = \frac{3\langle \Delta r^4 \rangle}{5\langle \Delta r^2 \rangle^2} - 1 \qquad (5)$$

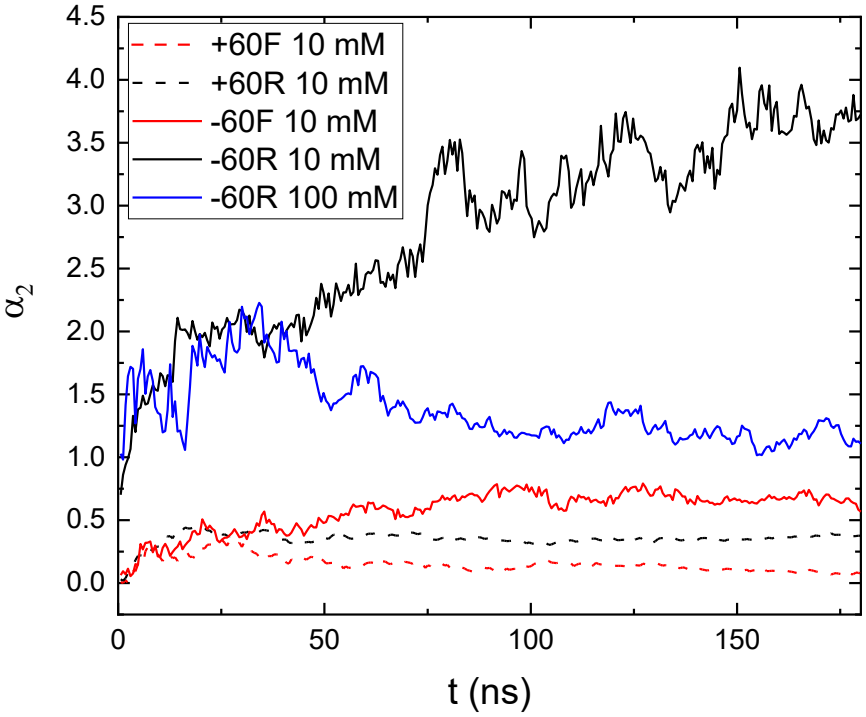

Figure 10. Non-Gaussian parameter (α_2) as a function of time for cases +60F, +60R, –60F and –60R at 10 mM (dashed red line, dashed black line, solid red line and solid black line, respectively) and –60R at 100 mM (blue solid line).

It can be shown that this parameter is zero for displacements with a normal probability density. Figure 10 displays α_2 (as a function of time) for the four representative cases

analyzed in this section. As can be seen, the solute displacements are largely Gaussian in three of the cases (+60F, +60R and −60F at 10 mM). However, the non-Gaussian parameter deviates significantly from zero for oppositely charged solutes in rigid gels (−60R) at 10 mM. This clearly agrees with the conclusion derived from the self-part of the Van Hove function. The simulations also reveal that diffusion deviates more from Gaussian behavior in rigid gels than in their flexible counterparts. A similar conclusion was reached from simulations of crosslinked gels[13] and gel-like system.[21] The behavior of −60R at 100 mM is somewhat more complex. At short times, the non-Gaussian grows very rapidly, as with −60R at 10 mM. However, after 25 ns, α_2 decreases slowly until it reaches a baseline close to 1. Samanta et al. have reported that the non-Gaussian parameter of rigid gel-like systems decreases at sufficiently long times.[21] This partly agree with our results for −60R at 100 mM but differs from that found at 10 mM.

3. Anomalous diffusion.

Now, let us pay attention to the exponent of anomalous diffusion. Figure 11 shows this parameter as a function of $Z_S Z_C$ for the four series at 100 mM. As can be seen, this graph is also asymmetric with respect to the *y*-axis. For repulsive electrostatic forces, the exponent deviates only slightly from unity, which means that anomalous diffusion is almost absent. In fact, some authors consider diffusive regimes those for which $n > 0.9$.[36] On the other hand, n clearly deviates from unity if $Z_S Z_C < 0$. However, it should be noted that the behavior of this exponent depends (at least to some extent) on flexibility: n is smaller for rigid gels. A similar conclusion has been reported for neutral gels.[13] In any case, the differences between rigid and flexible gels are more noticeable for $Z_S Z_C < -40$. In relation to the region of attractive electrostatic forces, it should also be mentioned that the n-values of the VCC series are somewhat smaller than those of the VSC series.

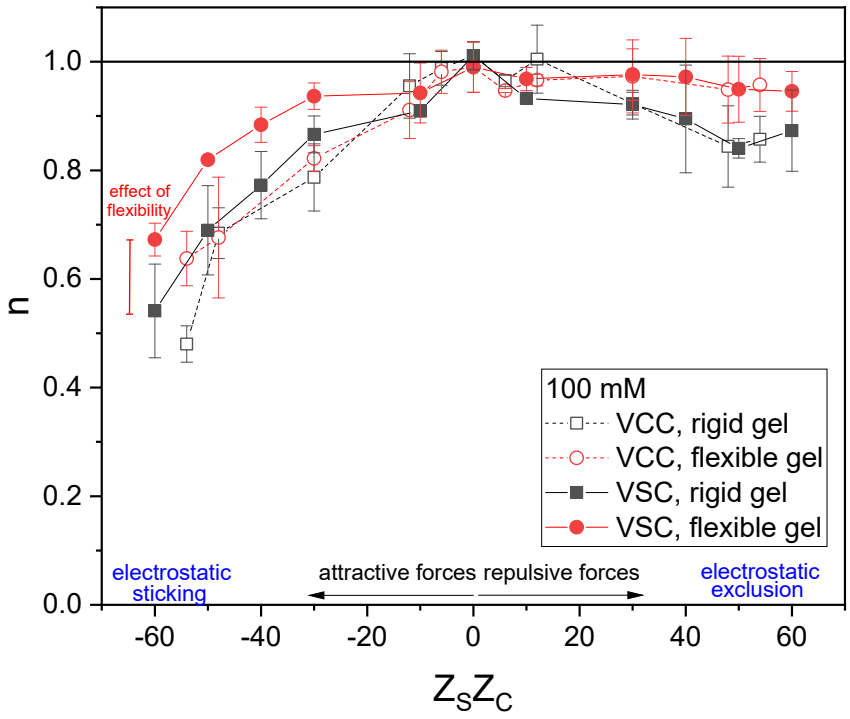

Figure 11. Exponent of anomalous diffusion (n) at 100 mM as a function of the product of charge numbers, $Z_S Z_C$. The graph includes series corresponding to variable chain charge (VCC) and variable solute charge (VSC) in flexible and rigid gels.

Figure 12 shows what happens to anomalous diffusion when the ionic strength is reduced to 10 mM. As can be seen on its right half, in this case n deviates slightly from unity for $Z_S Z_C > 0$. Quantitatively speaking, such a deviation is a bit larger than at 100 mM. Yet anomalous diffusion continues to be insignificant in the presence of repulsive electrostatic forces, mainly for flexible gels. The same qualitative trends as at 100 mM are also observed on the left side of the graph: i) the exponent is greater in flexible gels; ii) VCC series present smaller n-values than VSC series.

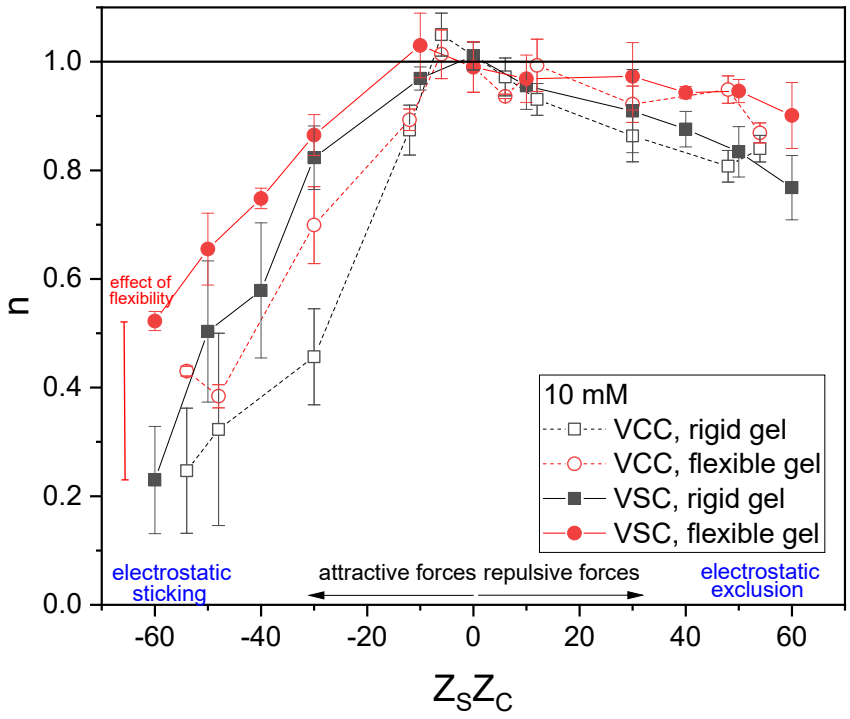

Figure 12. Exponent of anomalous diffusion (n) at 10 mM as a function of the product of charge numbers, $Z_S Z_C$. The graph includes series corresponding to variable chain charge (VCC) and variable solute charge (VSC) in flexible and rigid gels.

Xu *et al.* have experimentally observed the asymmetric behaviour of the anomalous diffusion exponent in the motion of polystyrene nanoparticles within bovine vitreous,[34] which is a negatively charged gel. Most of the n-values reported by these researchers for negatively charged nanoparticles are above 0.8, which is consistent with the right half of Figure 12. Only the larger particles present smaller exponents, which could be attributed to steric obstruction. On the contrary, the exponent is 0.20 for positively charged nanoparticles, in agreement with the left side of Figure 12.

Qualitatively speaking, the appearance of Figure 12 is very reminiscent of Figure 6. The effects of attractive and repulsive forces, flexibility and chain charge distribution are very similar in both figures. In fact, the anomalous diffusion exponent and the long-time

diffusion coefficient offer us complementary viewpoints (at different times) on the same effects.

CONCLUSIONS

In this work we have studied how electrostatic forces slow down the diffusion of the solute in a flexible gel. The coarse-grained model used explicitly considers flexible polyelectrolyte chains, which move according to a modified Brownian dynamics algorithm. The results are compared with those obtained for rigid networks to find out to what extent the effect of flexibility on electrostatic obstruction is important.

First, our data confirm that electrostatic obstruction in flexible gels is also charge asymmetric, which agrees previously reported results by other researchers from a very different model of network. This asymmetry is observed both in the long-time diffusion coefficient and in the exponent of anomalous diffusion. Attractive electrostatic forces slow down the movement of solute particles through the gel much more than the repulsive ones.

In any case, the model used here allows us to reach new conclusions regarding the flexibility of the polyelectrolyte chains. The diffusion coefficients obtained for flexible and rigid gels do not show important differences at 100 mM (except in the case of very intense attractive forces), but they do at 10 mM. This comparison thus reveals that flexibility facilitates diffusion if the ionic strength is low enough. In addition, it should be pointed out that anomalous diffusion is more pronounced in the case of rigid gels (even at 100 mM) and attractive electrostatic forces.

The model used here has also allowed us to explore what happens when the charge of the monomeric units varies discretely and not uniformly. In the case of attractive forces,

increasing the polyelectrolyte chain charge unevenly leads to greater electrostatic hindrance than increasing the solute charge.

Our simulations also show that in the case of very strong electrostatic attractive forces between the solute and the polyelectrolyte chains, the solute is preferentially localized in the vicinity of crosslinkers, both in rigid and flexible gels. However, solute motion exhibits very different features in these two cases. On the one hand, solute displacements are non-Gaussian in rigid gels. On the other hand, the fluctuations of the network in flexible gels allow solute particles to diffuse by occasionally jumping from crosslinker to crosslinker.

As mentioned above, one of the drawbacks of the Debye-Hückel potential is that it forces us to work with renormalized charges instead of the real ones. On the other hand, the validity of this potential is questionable in the presence of multivalent ions. Similar potentials based on linear approximations suffer from the same shortcomings. For these reasons, it would be interesting in the future to address the issue of electrostatic hindrance using primitive models.

Acknowledgements

The funding from "Consejería de Economía, Conocimiento, Empresas y Universidad, Junta de Andalucía, Programa Operativo FEDER Andalucía 2014-2020", Project P20_00138 and from "Ministerio de Ciencia e Innovación", Research network RED2022-134276-T, are gratefully acknowledged. In addition, A. M.-M. and M. M. R.-T. also thank the financial support by "Ministerio de Ciencia e Innovación", Projects PID2020-116615RA-I00 and PGC2018-098770-B-I00, respectively.

REFERENCES

[1] G.M. Geise, H.-S. Lee, D.J. Miller, B.D. Freeman, J.E. McGrath, and D.R. Paul, J. Polym. Sci. Part B Polym. Phys. **48**, 1685 (2010).

[2] G. Aggarwal and M. Nagpal, in *Polym. Gels Perspect. Appl.*, edited by V.K. Thakur, M.K. Thakur, and S.I. Voicu (Springer Singapore, Singapore, 2018), pp. 249–284.

[3] L. Lei, Y. Bai, X. Qin, J. Liu, W. Huang, and Q. Lv, Gels **8**, 301 (2022).

[4] O. Lieleg, I. Vladescu, and K. Ribbeck, Biophys. J. **98**, 1782 (2010).

[5] L. Johansson, U. Skantze, and J.E. Löfroth, J. Phys. Chem. **97**, 9817 (1993).

[6] T. Miyata, A. Endo, T. Ohmori, M. Nakaiwa, M. Kendo, K. Kurumada, and M. Tanigaki, J. Chem. Eng. JAPAN **35**, 640 (2002).

[7] T. Miyata, J. Phys. Soc. Japan **81**, 1 (2012).

[8] T. Stylianopoulos, M.-Z. Poh, N. Insin, M.G. Bawendi, D. Fukumura, L.L. Munn, and R.K. Jain, Biophys. J. **99**, 1342 (2010).

[9] X. Zhang, J. Hansing, R.R. Netz, and J.E. Derouchey, Biophys. J. **108**, 530 (2015).

[10] J. Hansing, C. Ciemer, W.K. Kim, X. Zhang, J.E. DeRouchey, and R.R. Netz, Eur. Phys. J. E **39**, 53 (2016).

[11] J. Hansing and R.R. Netz, Biophys. J. **114**, 2653 (2018).

[12] J. Hansing and R.R. Netz, Macromolecules **51**, 7608 (2018).

[13] M. Quesada-Pérez, J.A. Maroto-Centeno, M.D.M. Ramos-Tejada, and A. Martín-Molina, Macromolecules **55**, 1495 (2022).

[14] M. Quesada-Pérez, J.A. Maroto-Centeno, M. del M. Ramos-Tejada, and A. Martín-Molina, Phys. Chem. Chem. Phys. **23**, 14997 (2021).

[15] N. Kamerlin and C. Elvingson, J. Phys. Condens. Matter **28**, 475101 (2016).

[16] H.W. Cho, H. Kim, B.J. Sung, and J.S. Kim, Polymers (Basel). **12**, 2067 (2020).

[17] Y. Kim, S. Joo, W.K. Kim, and J.-H. Jeon, Macromolecules **55**, 7136 (2022).

[18] B.-R. Zhao and B. Li, J. Chem. Phys. **157**, 104901 (2022).

[19] W.K. Kim, R. Chudoba, S. Milster, R. Roa, M. Kanduč, and J. Dzubiella, Soft Matter **16**, 8144 (2020).

[20] S. Milster, W.K. Kim, M. Kanduč, and J. Dzubiella, J. Chem. Phys. **154**, 154902 (2021).

[21] N. Samanta and R. Chakrabarti, Soft Matter **12**, 8554 (2016).

[22] W.K. Kim, A. Moncho-Jordá, R. Roa, M. Kanduč, and J. Dzubiella, Macromolecules **50**, 6227 (2017).

[23] J. Shin, A.G. Cherstvy, and R. Metzler, Phys. Rev. X **4**, 21002 (2014).

[24] S.J. de Carvalho, R. Metzler, and A.G. Cherstvy, Phys. Chem. Chem. Phys. **16**, 15539 (2014).

[25] M. Quesada-Pérez, J. Callejas-Fernández, and R. Hidalgo-Álvarez, Adv. Colloid Interface Sci. **95**, 295 (2002).

[26] R.G. Winkler and A.G. Cherstvy, Phys. Rev. Lett. **96**, 066103 (2006).

[27] M. Quesada-Pérez, I. Adroher-Benítez, and J.A. Maroto-Centeno, J. Chem. Phys. **140**, 204910 (2014).

[28] M. Daeihamed, A. Haeri, S.N. Ostad, M.F. Akhlaghi, and S. Dadashzadeh, Nanomedicine **12**, 1187 (2017).

[29] D.L. Ermak, J. Chem. Phys. **62**, 4189 (1975).

[30] B. Cichoki and K. Hinsen, Physica A **166**, 473 (1990).

[31] R. Metzler, J.H. Jeon, A.G. Cherstvy, and E. Barkai, Phys. Chem. Chem. Phys. **16**, 24128 (2014).

[32] S.K. Ghosh, A.G. Cherstvy, and R. Metzler, Phys. Chem. Chem. Phys. **17**, 1847 (2015).

[33] A.G. Cherstvy, S. Thapa, C.E. Wagner, and R. Metzler, Soft Matter **15**, 2526 (2019).

[34] Q. Xu, N.J. Boylan, J.S. Suk, Y.-Y. Wang, E.A. Nance, J.-C. Yang, P.J. McDonnell,

R.A. Cone, E.J. Duh, and J. Hanes, J. Control. RELEASE **167**, 76 (2013).

[35] P. Kumar, L. Theeyancheri, S. Chaki, and R. Chakrabarti, Soft Matter **15**, 8992 (2019).

[36] J.S. Crater and R.L. Carrier, Macromol. Biosci. **10**, 1473 (2010).